



**HAL**  
open science

## Reactions of D<sub>2</sub> with 1,4-Bis(diphenylphosphino) butane-Stabilized Metal Nanoparticles-A Combined Gas-phase NMR, GC-MS and Solid-state NMR Study

Niels Rothermel, Tobias Röther, Tuğçe Ayvalı, Luis Miguel Martinez-Pietro, Karine Philippot, Hans-heinrich Limbach, Bruno Chaudret, Torsten Gutmann, Gerd Buntkowsky

### ► To cite this version:

Niels Rothermel, Tobias Röther, Tuğçe Ayvalı, Luis Miguel Martinez-Pietro, Karine Philippot, et al.. Reactions of D<sub>2</sub> with 1,4-Bis(diphenylphosphino) butane-Stabilized Metal Nanoparticles-A Combined Gas-phase NMR, GC-MS and Solid-state NMR Study. *ChemCatChem*, 2019, 11 (5), pp.1465-1471. 10.1002/cctc.201801981 . hal-02140624

**HAL Id: hal-02140624**

**<https://hal.science/hal-02140624v1>**

Submitted on 9 Dec 2020

**HAL** is a multi-disciplinary open access archive for the deposit and dissemination of scientific research documents, whether they are published or not. The documents may come from teaching and research institutions in France or abroad, or from public or private research centers.

L'archive ouverte pluridisciplinaire **HAL**, est destinée au dépôt et à la diffusion de documents scientifiques de niveau recherche, publiés ou non, émanant des établissements d'enseignement et de recherche français ou étrangers, des laboratoires publics ou privés.

# Reactions of D<sub>2</sub> with 1,4-Bis(diphenylphosphino)butane stabilized Metal Nanoparticles – A combined gas-phase NMR, GC-MS and solid-state NMR Study

Niels Rothermel<sup>a</sup>, Tobias Röther<sup>a</sup>, Tugce Ayvali<sup>b</sup>,  
Luis M. Martínez-Prieto<sup>b</sup>, Karine Philippot<sup>b</sup>, Hans-Heinrich Limbach<sup>c, a</sup>, Bruno  
Chaudret<sup>d\*</sup>, Torsten Gutmann<sup>a\*</sup>, Gerd Buntkowsky<sup>a\*</sup>

<sup>a</sup>TU Darmstadt; Eduard-Zintl-Institut für Anorganische und Physikalische Chemie, Alarich-Weiss-  
Straße 4,

D-64287 Darmstadt, Germany

<sup>b</sup>LCC-CNRS Université de Toulouse; CNRS; 205 Route de Narbonne,

F-31077 Toulouse, France

<sup>c</sup>Freie Universität Berlin; Institut für Chemie und Biochemie, Takustr. 3, D-14195 Berlin, Germany

<sup>d</sup>Université de Toulouse; INSA, UPS, CNRS; LPCNO, 135 avenue de Rangueil, F-31077 Toulouse, France

\* Corresponding authors:

[gerd.buntkowsky@chemie.tu-darmstadt.de](mailto:gerd.buntkowsky@chemie.tu-darmstadt.de),

[gutmann@chemie.tu-darmstadt.de](mailto:gutmann@chemie.tu-darmstadt.de),

[chaudret@insa-toulouse.fr](mailto:chaudret@insa-toulouse.fr)

## Abstract

The reactions of three metal nanoparticle (MNP) systems Ru/dppb, RuPt/dppb, Pt/dppb (dppb = 1,4-bis(diphenylphosphino)butane) with gaseous D<sub>2</sub> at room temperature and different gas pressures have been studied using <sup>1</sup>H gas phase NMR, GC-MS and solid state <sup>13</sup>C and <sup>31</sup>P MAS NMR. The main product is gaseous HD arising from the reaction of D<sub>2</sub> with surface hydrogen sites created during the synthesis of the nanoparticles. In a side reaction, some of the dppb ligands are decomposed producing surface phosphorus species and gaseous partially deuterated butane and cyclohexane. These findings are fundamental for detailed studies of the reaction kinetics of these particles towards H<sub>2</sub> or D<sub>2</sub> gas.

## 1 Introduction

Nanoparticles of transition metals, stabilized by organic ligands, are an interesting class of catalysts, since they represent a hybrid between a heterogeneous and a homogeneous catalyst. The combination of both fields is important for hydrogenations of arenes under mild conditions.<sup>1-2</sup> In comparison to classical heterogeneous catalysts, such as zeolite-supported noble metals used for aromatic hydrogenations,<sup>3</sup> metal nanoparticles offer many possibilities for fine tuning with respect to activity and selectivity due to their stabilizing ligand system. This makes it possible to modify nanoparticles not only for operations in different solvents such as aromatics, alcohols and even water, but also for

1 stereoselective operations.<sup>4</sup> Particles tuned in this way have been recently used for the regioselective  
2 and stereo specific deuteration of a wide range of bioactive aza compounds.<sup>5-6</sup>

3 To design metal nanoparticle systems that fulfill the high demands on activity and selectivity of modern  
4 catalysis, it is crucial to gain a deeper understanding of the processes that take place on the  
5 nanoparticle surface during the catalytic reaction. For the characterization of surface species and the  
6 observation of surface processes on metal nanoparticles (MNPs), solid state and gas phase NMR have  
7 proven to be valuable spectroscopic methods.<sup>7-11</sup> For MNPs formed by hydrogenation of  
8 organometallic precursors it has been shown by a combination of <sup>1</sup>H gas phase and solid state <sup>2</sup>H NMR  
9 that hydrides are present on the surface of the particles and that they are mobile and exchangeable  
10 by deuterium.<sup>12</sup> Recently, some of us have explored the kinetics of gas-solid hydrogen isotope  
11 exchange of ruthenium metal nanoparticles (RuMNPs) in more detail.<sup>13</sup> It was found that when D<sub>2</sub> is  
12 applied to the latter, a direct reaction with surface hydrides occurs without D<sub>2</sub> dissociation leading to  
13 the formation of HD in the initial reaction stages.  
14  
15  
16

17 Whereas we have studied previously RuMNPs containing different stabilizing ligand systems, namely  
18 Ru/PVP (PVP = polyvinylpyrrolidone) and Ru/HDA (HDA = hexadecylamine), we have investigated in  
19 the present work the more reactive Ru/dppb system (**1**) (dppb = 1,4-bis(diphenylphosphino)butane)  
20 at 1 and 2 bar D<sub>2</sub> pressures. As we also wanted to explore the role of the metal, we studied as well the  
21 bimetallic system of ruthenium and platinum RuPt/dppb (**2**) and the monometallic system of platinum  
22 Pt/dppb (**3**). In the course of our studies we observed a hydrogenation of the phenyl groups of dppb  
23 and a partial decomposition of the ligand system that leaves into the gas phase. Therefore, the  
24 composition of the gas phase has been further analyzed in detail by GC-MS. Finally, multinuclear solid-  
25 state NMR experiments have been used to evaluate the impact of hydrogen gas on the structure of  
26 the particles' ligand shell.  
27  
28  
29  
30  
31  
32  
33  
34  
35

## 36 **2 Experimental Section**

### 37 **2.1 General**

38 All reactions were carried out using Schlenk or Fisher-Porter bottle techniques under an inert and dry  
39 atmosphere. THF was distilled over CaH<sub>2</sub> and pentane over sodium. The solvents were degassed by  
40 means of three freeze-pump cycles. 1,4-bis(diphenylphosphino)butane (dppb) was purchased from  
41 Sigma-Aldrich - and (Cyclo-octadiene)(cyclo-octatriene)ruthenium(0) (Ru(COD)(COT)) for the synthesis  
42 of Ru/dppb (**1**) from Umicore. For RuPt/dppb (**2**) the Ru(COD)(COT) precursor was purchased from  
43 Nanomeps (Toulouse), dibenzylideneacetone (dba) from Alfa-Aesar and Pt(CH<sub>3</sub>)<sub>2</sub>(COD) from Strem and  
44 used without further purification. D<sub>2</sub> (99.82%) gas for the exchange reactions was purchased from  
45 Eurisotop.  
46  
47  
48  
49  
50

### 51 **2.2. Synthesis**

52 The synthesis of all three nanoparticle systems followed the organometallic approach described in the  
53 literature,<sup>9-10, 14</sup> where transition metal complexes containing unsaturated ligands are hydrogenated  
54 using gaseous H<sub>2</sub> in dilute solutions of THF at room temperature, in the presence of a sub-  
55 stoichiometric amount of dppb.  
56  
57  
58  
59  
60  
61  
62  
63  
64  
65

### 2.2.1. Ru/dppb (1)

200 mg of Ru(COD)(COT) (0.634 mmol) were introduced in a Fisher-Porter bottle and left in vacuum for 30 min. 120 mL of freshly distilled THF was then added and the resulting yellow solution was cooled to 193 K. Under rigorous stirring, a solution of 27 mg (0.0633 mmol, 0.1 eq.) dppb in 80 mL THF was slowly added to the precursor solution. The Fisher-Porter bottle was pressurized with 3 bar of H<sub>2</sub> gas and the solution was left to slowly reach room temperature (r.t.) under continuous stirring. After 18 h of reaction a black colloidal solution was obtained. The solvent was removed in vacuum to reach a volume of approximately 10 mL. To this solution 80 mL of pentane were added. After 1 h a black precipitate was formed and the solvent was removed by filtration. The black precipitate was further washed with 2 x 35 mL pentane and dried at room temperature under vacuum over night to yield Ru/dppb (1) particles as a black powder.

### 2.2.2. RuPt/dppb (2)

142 mg of Ru(COD)(COT) (0.451 mmol) and 150 mg of Pt(CH<sub>3</sub>)<sub>2</sub>(COD) (0.451 mmol) were introduced into a Fisher-Porter bottle and dissolved in 100 mL THF. The so-obtained yellow solution was cooled to 213 K and a solution of 93.2 mg (0.226 mmol, 0.25 eq.) dppb in 80 mL THF was added under rigorous stirring. After pressurization with 3 bar H<sub>2</sub> the solution was left to reach r.t. under continuous stirring. After 18 h the black colloidal solution was reduced to a volume of approximately 10 mL under vacuum. Afterwards 40 mL of cold pentane (243 K) were added to precipitate the particles. The solvent was removed by filtration and the resulting black solid powder was washed with 2 x 40 mL of pentane. The product was dried under vacuum overnight, yielding RuPt/dppb (2) particles.

### 2.2.3. Pt/dppb (3)

300 mg of Pt(dpa)<sub>2</sub> (0.452 mmol) were dissolved in 170 mL THF in a Fisher-Porter bottle. The obtained purple black solution was cooled to 243 K and a solution of 38.6 mg (0.0905 mmol, 0.2 eq.) dppb in 10 mL THF was added under stirring. The mixture was then pressurized with 3 bar of H<sub>2</sub> gas and left to slowly reach r.t. under continuous stirring. After 24 h of reaction, the black colloidal solution was reduced to a volume of approximately 20 ml in vacuum and 30 mL of cold pentane were added for a quick precipitation of a black solid. The solvent was removed by filtration and the product was further washed with 6 x 30 mL of cold pentane. The product was dried under vacuum overnight, yielding Pt/dppb (3) particles.

## 2.3. Characterization techniques

### 2.3.1. Gas Phase NMR

<sup>1</sup>H gas-phase NMR spectra were recorded on a Bruker Avance III HD 500 spectrometer at 11.7 T corresponding to a frequency of 500.26 MHz for <sup>1</sup>H. This system is equipped with a Bruker DUL 500 MHz S2 5 mm Probe.

10 mg of the corresponding nanoparticles (1-3) were filled into a sealable pressure resistant NMR sample tube (Wilmad Lab-Glass Quick Pressure Valve NMR Sample Tube, 2.51 mL inner volume). The sample tube was evacuated for at least 30 min before connection to a D<sub>2</sub> gas bottle via PFA tubing. The D<sub>2</sub> pressure was adjusted to 1 bar (1a-3a) or 2 bar (1b-3b), respectively, and the Teflon seal of the

1 evacuated sample tube was opened quickly to apply a D<sub>2</sub> atmosphere to the particles. The tube was  
2 sealed again and directly put into the spectrometer to record <sup>1</sup>H NMR spectra of the gas phase  
3 containing an assumed mixture of H<sub>2</sub>, HD, D<sub>2</sub> and volatile solvent molecules.

### 4 **2.3.2. Gas Chromatography and Mass Spectrometry**

5 For RuPt/dppb nanoparticles an analysis of the gas-phase was performed by GC-MS. Experiments were  
6 performed on a Fisons MD 800 mass spectrometer equipped with a quadrupole detector and a DB-5  
7 column. For the measurement a sample of 12.6 mg RuPt/dppb was treated with 3 bar D<sub>2</sub> at r.t. (**2c**)  
8 and stored for 7 days. The injector was heated to 240°C and a volume of 200 μL of the gas-phase above  
9 the RuPt/dppb was injected. A temperature ramp (40°C for 10 min, heating 25°C/min to 150°C, keeping  
10 150°C for 2 min) and He as carrier gas was chosen to separate the different side products that were  
11 analyzed by MS.  
12  
13  
14  
15

### 16 **2.3.3. Solid State NMR**

17 <sup>13</sup>C and <sup>31</sup>P CP MAS experiments were recorded on a Bruker Avance III spectrometer at 7 T  
18 corresponding to a frequency of 75.47 MHz for <sup>13</sup>C and 121.49 MHz for <sup>31</sup>P respectively. This system is  
19 equipped with a 4 mm H/X probe. All experiments were performed at spinning rates of 8 kHz and  
20 repetition delays of 4 s. The spectra were recorded utilizing ramped CP MAS sequences.<sup>15</sup> For <sup>13</sup>C and  
21 <sup>31</sup>P, contact times were set to 3 and 3.2 ms, respectively. Two sets of experiments were performed.  
22 One set was performed on the Ru/dppb particles (**1**) directly after they were synthesized. The other  
23 set was performed after treating the same sample with hydrogen gas (RuH/dppb (**1c**)). The sample  
24 preparation constituted of three overnight treatments with 1.5 bar H<sub>2</sub> and two intraday treatments  
25 with 1.5 bar H<sub>2</sub> for 2 h. After each treatment, the sample was exposed to vacuum for at least 30 min  
26 to remove decomposition products of the ligands.  
27  
28  
29  
30  
31  
32  
33  
34  
35

## 36 **3. Results and Discussion**

### 37 **3.1. Gas Phase Measurements**

38 In Figure 1 are depicted typical <sup>1</sup>H gas-phase NMR spectra obtained for all three particle systems after  
39 16 h exposure to 1 bar (**1a-3a**) or 2 bar (**1b-3b**) D<sub>2</sub> at room temperature. All spectra show a signal at  
40 4.5 ppm arising from gaseous dihydrogen. By line shape analysis (**1d**, see ESI Figure S1) a line width of  
41 about 180 Hz is obtained which corresponds to the one of HD, *i.e.* the amount of H<sub>2</sub> is negligible as it  
42 exhibits a much broader line width (see ESI Figure S2 and ref. 13). This result is corroborated by the  
43 Raman spectrum (**1e**, ESI Figure S3) recorded for the gas-phase upon reaction of D<sub>2</sub> with the particles,  
44 where H<sub>2</sub> is barely observable, in contrast to the vibrations of HD and D<sub>2</sub>.  
45  
46  
47  
48  
49  
50  
51

52 In addition to HD as main reaction product, the spectra in Figure 1 reveal the formation of side products  
53 giving rise to signals at high field between 0 and 1.5 ppm. This region is typical for alkanes which must  
54 have been formed by reaction of D<sub>2</sub> with the dppb ligands. That reaction is corroborated for Pt/dppb  
55 sometimes by the observation of a thin film of a liquid, condensing at the inner wall of the NMR tube  
56 when the D<sub>2</sub> gas is applied for sample preparation.  
57  
58

59 We assign these alkane signals as follows. The signal at 1.5 ppm is typical for cyclohexane<sup>16</sup> and those  
60 at 1.35 ppm and 0.95 ppm for the methylene and methyl groups of butane.<sup>17</sup> Furthermore, in contrast  
61  
62  
63  
64  
65

to the Pt-containing NPs, the spectra of the Ru-containing NPs present an additional signal around 0.2 ppm. That is the chemical shift of methane.<sup>18</sup> From Fig.1 it is evident that the Pt and Ru containing NPs exhibit a different pressure dependence. In case of the Pt/dppb NPs, the alkane signals grow with pressure and in case of the Ru-containing NPs, the alkane signals are weakened with growing pressure. This is a clear indication that the H/D exchange in the alkane moieties of the ligand is more efficient in the Ru/dppb NPs.

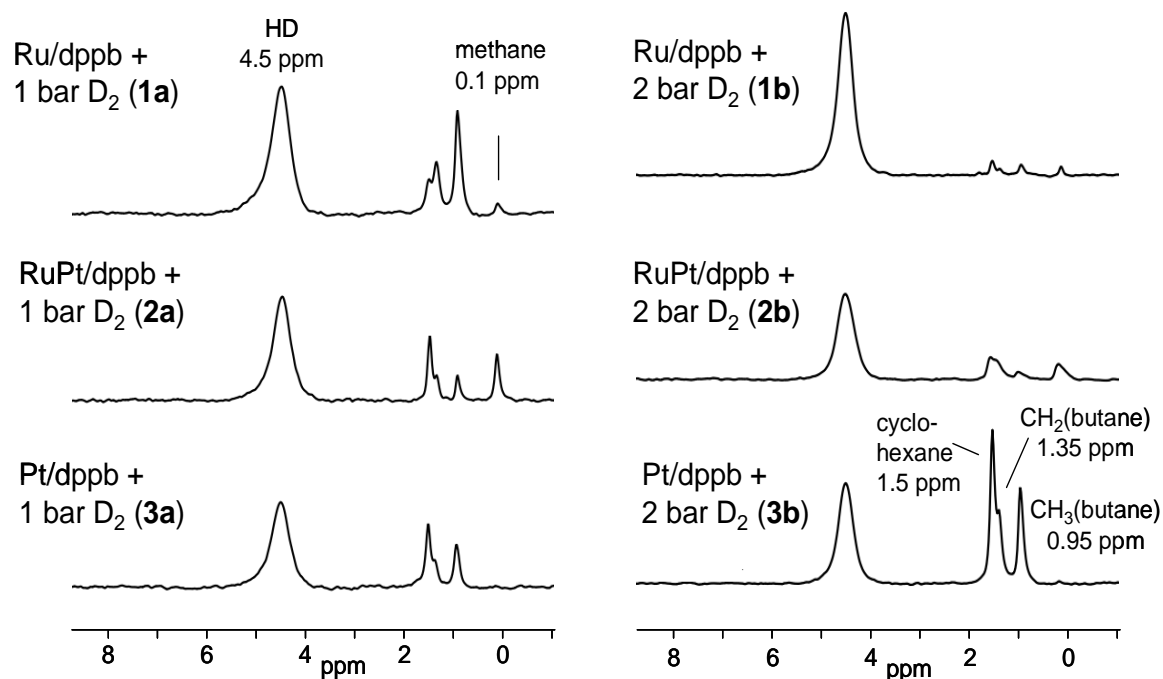
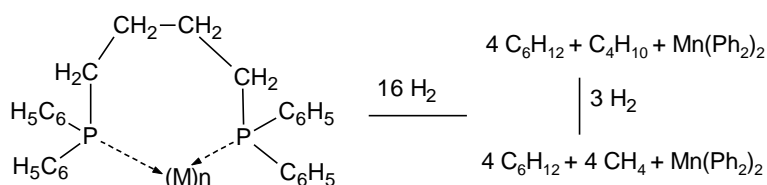


**Figure 1:** Typical  $^1\text{H}$  gas-phase NMR spectra after exposing solid MNPs at room temperature to 1 bar (**1a-3a**) or 2 bar (**1b-3b**)  $\text{D}_2$  gas for 16 h. The chemical shift of the HD signal is set to 4.5 ppm. For comparison of the signal intensities of the different particle systems, all spectra were processed using the same parameters.

As the alkanes formed from Ru/NPs will be partially deuterated, one might expect that part of the corresponding alkane signals experience small high field shifts. Indeed, we observe in the 2 bar  $\text{D}_2$  experiments with Ru-containing NPs that signals of the alkanes released into the gas phase contain high-field shoulders. Therefore, we checked whether these shoulders could arise from H/D isotope effects which lead to high-field shifts of the remaining carbon bound H nuclei. In the case of methane in organic solvents a high-field shift of about 0.045 ppm was observed for  $\text{CH}_4/\text{CHD}_3$ , which depended on the type of solvent and on temperature.<sup>19</sup> However, the shoulders which we observe seem to arise from somewhat larger shifts, their exact value being difficult to obtain. Another explanation would be that some of the alkanes at high pressure are not located in the gas phase but interacting with the particles, either adsorbed or in rapid gas-surface exchange, or as tiny droplets.

Finally, we note that in the case of RuPt/dppb the amount of obtained butane is reduced as compared to Ru/dppb, but the amount of methane increased, as expected for more efficient C-C bond breaking processes.

For the above mentioned MNPs, the alkane side products must be formed by the reaction of the dppb ligands at particularly reactive sites. The following reaction scheme is conceivable.



**Scheme 1.** Hydrogenation and alkane release of a metal dppb ligand by dihydrogen. The phosphine species formed may not be stable but subject to further reactions, in particular with oxygen.

Scheme 1 suggests the formation of metal bound PH<sub>2</sub> surface species, but the latter might easily oxidize. In order to know the details of these reactions extended kinetic and computational studies are required which were beyond the scope of this work.

### 3.2. GC-MS Measurements

For the detailed characterization of the reaction products, gas-chromatography coupled to mass spectrometry (GC-MS) was applied. As example, RuPt/dppb was treated with 3 bar D<sub>2</sub> gas pressure (**2c**) to produce a higher amount of side products for analysis. RuPt/dppb (**2**) was chosen because it does not tend to quench the reaction compared to Pt/dppb (**3**) but it produces larger amounts of side product than Ru/dppb (**1**).

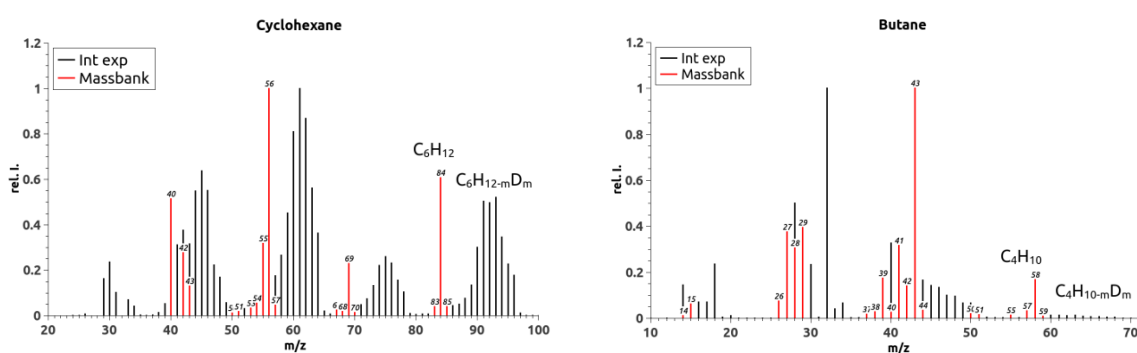


**Figure 2:** Recorded mass spectra of the cyclohexane and the butane fraction of the H/D exchange reaction with RuPt/dppb performed with 3 bar initial D<sub>2</sub> gas pressure (**2c**). The red signals represent the mass spectrum of the individual species with natural isotope distribution as found in a mass database.

1 Two main fractions were separated (Figure 2) that are clearly attributed to cyclohexane and butane  
2 according to their spectra pattern. This is in excellent agreement with the  $^1\text{H}$  gas phase NMR of **1a** and  
3 **1b** (Figure 1), which show the signals of these compounds in the aliphatic region. The appearance of  
4 butane and cyclohexane illustrates that the particles facilitate the cleavage of the C-P bond upon  
5 decomposition of the dppb ligand, similar to related phosphido bridged transition metal cluster  
6 complexes.<sup>20-22</sup>  
7

8 The spectrum of the cyclohexane fraction in Figure 2 shows a “broadening” of the mass distribution  
9 compared to the spectrum of pure cyclohexane. The location of the molecular peak at  $m/z = 84$  is  
10 shifted to higher  $m/z$  values between 84 and 96. This is a clear hint that deuterium is incorporated into  
11 the aliphatic parts of the ligand. Similar results are also observed for the fraction of butane (Figure 2).  
12 This observation is in excellent agreement with the deuteration of alkanes on Ru/dppb MNPs as  
13 demonstrated in our previous work.<sup>23</sup>  
14  
15  
16

17 Comparing the mole peak of the mass spectrum of cyclohexane and the one from butane ( $m/z$  value  
18 of 58+), one notices a narrower distribution of masses in the case of cyclohexane and a more extensive  
19 deuteration. This phenomenon can be explained by different deuteration mechanisms. Due to the  
20 aromatic nature of the dppb ligand, some deuterons are incorporated by direct hydrogenation of the  
21 aromatic rings or already cleaved benzene.<sup>24-26</sup> This leads to the formation of cyclohexane or partly  
22 hydrogenated respectively deuterated C6 analogues. Furthermore, fully deuteration of the  
23 cyclohexane and C6 analogues is feasible as shown by the isotopomer patterns for the deuteration of  
24 benzene or toluene (ESI Figure S4). This would require a C-H bond activation on the surface of the  
25 particles.  
26  
27  
28  
29

30 Deuteration of the butane fragment on the other hand, is only feasible through C-H-bond activation  
31 on the metal surface and not by direct reaction. Such C-H-bond activation is favored as long as the  
32 butane moiety is in close proximity to the surface which is highly probable when it is linked to  
33 phosphorus that coordinates to the surface. Based on liquid state NMR studies on alkylamine-  
34 stabilized Ru NPs, it was previously suggested that the presence of such an agostic interaction may  
35 lead to the deuteration of alkylic species as in the present case.<sup>11</sup>  
36  
37  
38  
39  
40

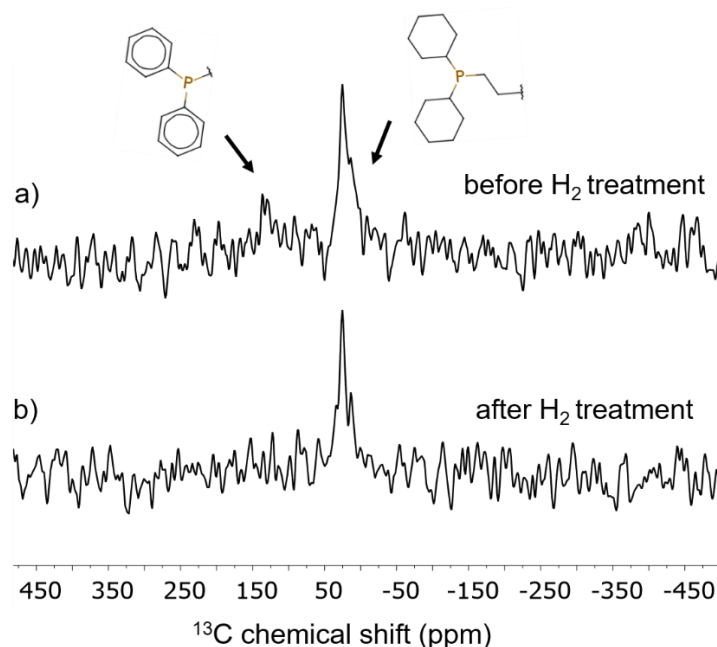
### 41 **3.3. Solid State NMR**

42 The fate of the dppb ligands of Ru/dppb, RuPt/dppb and Pt/dppb was indirectly elucidated by GC-MS  
43 analysis of the side products formed when the particles are exposed to  $\text{D}_2$  gas. The next step was to  
44 study the change of the NP surface structure, when the dppb ligand is transformed. Through the  
45 observation of cyclohexane and butane in the side product fraction, the phosphorus moieties are likely  
46 transformed into metal bound phosphanes ( $-\text{PH}_x\text{C}_{3-x}$ ). To shed more light on the structural changes,  $^{13}\text{C}$   
47 and  $^{31}\text{P}$  CP MAS NMR measurements were performed before and after hydrogen treatment (Ru/dppb  
48 (**1**) and RuH/dppb (**1c**)).  
49  
50  
51  
52

53 The  $^{13}\text{C}$  CP MAS spectra of Ru/dppb recorded before and after treatment with  $\text{H}_2$  gas (Figure 3a,b) both  
54 feature signals of aliphatic carbons located around 25 ppm. Before the treatment, a small signal at 130  
55 ppm is visible that is attributed to phenyl groups of non-hydrogenated dppb ligands. This weak  
56 aromatic signal in dppb based particles varies in intensity between different particle samples. The  
57 intensity can for example be affected by storage time and also by small experimental deviations. In  
58 addition to that, the measurement shows that not all ligands on the metal surface undergo  
59  
60  
61  
62  
63  
64  
65



1 decomposition but all aromatic species are hydrogenated. Ligands that undergo decomposition could  
2 therefore be located at very reactive sites on the metal surface. Based on previous surface studies with  
3 CO adsorbed on Ru/dppb it is assumed that ligands are located on apexes of the particle.<sup>9</sup> The observed  
4 decomposition products most probably stem from ligands which are not located on apex positions and  
5 are therefore labile and readily react with hydrides in their vicinity.  
6  
7



8  
9  
10  
11  
12  
13  
14  
15  
16  
17  
18  
19  
20  
21  
22  
23  
24  
25  
26  
27  
28  
29 **Figure 3:** <sup>13</sup>C CP MAS spectra measured at 8 kHz spinning of Ru/dppb measured before (a) and after (b)  
30 treatment with H<sub>2</sub> gas.  
31

32  
33  
34 The <sup>31</sup>P CP MAS spectra of Ru/dppb recorded before and after treatment with H<sub>2</sub> gas (Figure 4a,b),  
35 show clear differences in their line shape and an improved resolution and S/N ratio is obtained after  
36 H<sub>2</sub> treatment. The better resolution and S/N ratio seem to be the consequence of the saturation of the  
37 metal surface with hydrogen upon H<sub>2</sub> treatment, which improves the cross-polarization efficiency.  
38 Nevertheless, no additional signals appeared after treatment with H<sub>2</sub> gas, which indicates that no  
39 significant changes of the structure occurred during the H<sub>2</sub> treatment.  
40  
41  
42  
43  
44  
45  
46  
47  
48  
49  
50  
51  
52  
53  
54  
55  
56  
57  
58  
59  
60  
61  
62  
63  
64  
65

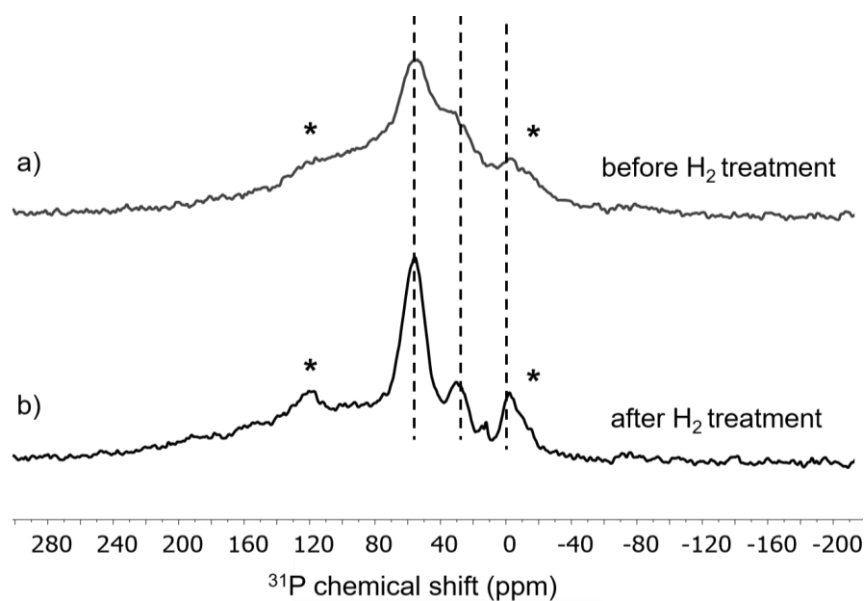


**Figure 4:**  $^{31}\text{P}$  CP MAS spectra measured at 8 kHz spinning of Ru/dppb measured before (a) and after (b) treatment with  $\text{H}_2$  gas. Note that signals marked with asterisks are spinning sidebands of the signal at ca. 56 ppm.

An assignment of individual signals has to be done with care. Following previous  $^{31}\text{P}$  solid state NMR studies<sup>24</sup> the major signal located at 56 ppm is most probably attributed to phosphine species coordinated to the metal surface. Based on the characterization of the dppb chemistry towards decomposition and hydrogenation, a range of different phosphine species is expected to be present on the surface, i.e. *alkyl-P(Ph/Cy)<sub>2</sub>*, *alkyl-P(Ph/Cy)H*, *alkyl-PH<sub>2</sub>*,  $\text{H}_n\text{P}(\text{Ph/Cy})_{3-n}$  and arene hydrogenation products from all these species, which are not fully hydrogenated to cyclohexyl. Based on the  $^{13}\text{C}$  spectra it can be assumed that arene phosphines are the least dominant surface species. The signal located at 29 ppm seems to correspond to co-adsorbed phosphine oxides.

### 3.4. Reactions on dppb stabilized nanoparticles

The results of the previous sections reveal a clearer picture on the surface reactions of dppb stabilized MNPs. For the details of the formal reactions of the dppb ligands with  $\text{H}_2$  or  $\text{D}_2$  (Scheme 1) we discuss some possible mechanisms depicted in Figure 5. Gaseous  $\text{H}_2$  or  $\text{D}_2$  are consumed and as main products butane and cyclohexane are formed as proven by NMR and GC-MS analysis of the gas phase. On the other hand, some dppb ligands remain as partially hydrogenated/deuterated ligands on the surface as evidenced by  $^{13}\text{C}$  and  $^{31}\text{P}$  solid-state NMR.

Together with the results from our former paper on alkane deuteration<sup>23</sup> a variety of side reactions can be identified as illustrated in Figure 5. The reaction steps A1 and A2 describe the C-P bond cleavage catalyzed by the particle that leads to the formation of benzene and butane. The details of these complex reaction steps are illustrated in Figure S5 in the ESI. In step B, benzene reacts further to form cyclohexane. In step C1 and C2, cyclohexane or butane are deuterated by C-H bond activation on the particle surface. In addition to the reactions that involve the dppb ligand,  $\text{D}_2$  is adsorbed on the surface and is transformed into surface deuterides in step D. Surface deuterides scramble with surface hydrides and form HD that can leave the particle due to the surface/gas phase equilibrium in step E. Finally, in a step F the hydrogenation of the dppb is feasible which leads to 1,4-Bis(dicyclohexylphosphino)butane in case of total hydrogenation.

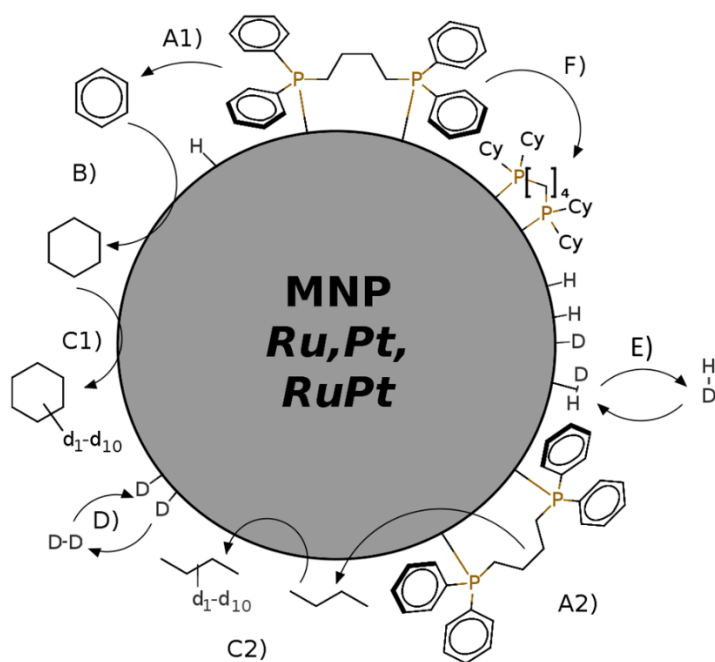


**Figure 5:** Reactions taking place on dppb stabilized nanoparticles when exposed to D<sub>2</sub>.

## 4. Conclusions

Three 1,4-Bis(diphenylphosphino)butane stabilized nanoparticle systems (Ru/dppb, Pt/dppb and RuPt/dppb) were investigated in the reaction with D<sub>2</sub> gas. Next to HD exchange with gaseous dihydrogen isotopomers, these particle systems were found to be capable of catalyzing the deuteration of aliphatic substrates. The latter was confirmed by GC-MS analysis of the gas phase after reaction with D<sub>2</sub> gas, which allowed a detailed characterization of the side products that were observed in the <sup>1</sup>H gas phase NMR spectra. The formation of deuterated butane and cyclohexane isotopomers revealed that all three particle systems not only catalyze an isotope exchange but also catalyze P-C bond cleavage reactions of their dppb ligands in very mild reaction conditions. Exemplary, <sup>13</sup>C and <sup>31</sup>P solid state NMR experiments on Ru/dppb show that even after multiple hydrogen treatments, which trigger the decomposition of the dppb ligand, the latter remains on the particle surface. These results demonstrate that the surface composition is not drastically influenced by this decomposition reaction. For deeper studies of HD exchange kinetics, it is however necessary to pretreat the particles with H<sub>2</sub> gas to gain reproducible initial conditions for the surface reaction.

## 5. Acknowledgements

This research was supported by the Deutsche Forschungsgemeinschaft under contract Bu-911-19-1/2 (DFG-ANR project MOCA-NANO): The authors thank Christiane Rudolph, Gül Sahinalp and Alexander Schießer of the mass spectrometry department of TU Darmstadt for their technical support.

## References

1. Debouttière, P.-J.; Coppel, Y.; Denicourt-Nowicki, A.; Roucoux, A.; Chaudret, B.; Philippot, K., PTA-Stabilized Ruthenium and Platinum Nanoparticles: Characterization and Investigation in Aqueous Biphasic Hydrogenation Catalysis. *European Journal of Inorganic Chemistry* **2012**, (8), 1229-1236.
2. Widegren, J. A.; Finke, R. G., A review of soluble transition-metal nanoclusters as arene hydrogenation catalysts. *Journal of Molecular Catalysis A: Chemical* **2003**, *191* (2), 187-207.
3. Stanislaus, A.; Cooper, B. H., Aromatic Hydrogenation Catalysis: A Review. *Catalysis Reviews* **1994**, *36* (1), 75-123.
4. Jansat, S.; Picurelli, D.; Pelzer, K.; Philippot, K.; Gómez, M.; Muller, G.; Lecante, P.; Chaudret, B., Synthesis, characterization and catalytic reactivity of ruthenium nanoparticles stabilized by chiral N-donor ligands. *New Journal of Chemistry* **2006**, *30* (1), 115-122.
5. Pieters, G.; Taglang, C.; Bonnefille, E.; Gutmann, T.; Puente, C.; Berthet, J.-C.; Dugave, C.; Chaudret, B.; Rousseau, B., Regioselective and stereospecific deuteration of bioactive aza compounds by the use of ruthenium nanoparticles. *Angew. Chem. Intl. Ed.* **2014**, *53* (1), 230-234.
6. Taglang, C.; Martinez-Prieto, L. M.; del Rosal, I.; Maron, L.; Poteau, R.; Philippot, K.; Chaudret, B.; Perato, S.; Lone, A. S.; Puente, C.; Dugave, C.; Rousseau, B.; Pieters, G., Enantiospecific CH Activation Using Ruthenium Nanocatalysts. *Angew. Chem., Int. Ed.* **2015**, *54* (36), 10474-10477.
7. Gutmann, T.; Del Rosal, I.; Chaudret, B.; Poteau, R.; Limbach, H.-H.; Buntkowsky, G., From Molecular Complexes to Complex Metallic Nanostructures-(2) H Solid-State NMR Studies of Ruthenium-Containing Hydrogenation Catalysts. *Chem. Phy. Chem.* **2013**, *14*, 3026-3033.
8. Gutmann, T.; Del Rosal, I.; Chaudret, B.; Poteau, R.; Limbach, H.-H.; Buntkowsky, G., From Molecular Complexes to Complex Metallic Nanostructures-(2) H Solid-State NMR Studies of Ruthenium-Containing Hydrogenation Catalysts. *ChemPhysChem : a European journal of chemical physics and physical chemistry* **2013**, *14*, 3026-3033.
9. Novio, F.; Philippot, K.; Chaudret, B., Location and Dynamics of CO Coordination on Ru Nanoparticles: A Solid State NMR Study. *Catal. Lett.* **2010**, *140* (1-2), 1-7.
10. Kinayyigit, S.; Lara, P.; Lecante, P.; Philippot, K.; Chaudret, B., Probing the surface of platinum nanoparticles with <sup>13</sup>CO by solid-state NMR and IR spectroscopies. *Nanoscale* **2014**, *6* (1), 539-46.
11. Pan, C.; Pelzer, K.; Philippot, K.; Chaudret, B.; Dassenoy, F.; Lecante, P.; Casanove, M. J., Ligand-stabilized ruthenium nanoparticles: synthesis, organization, and dynamics. *Journal of the American Chemical Society* **2001**, *123* (31), 7584-93.
12. Pery, T.; Pelzer, K.; Buntkowsky, G.; Philippot, K.; Limbach, H.-H.; Chaudret, B., Direct NMR evidence for the presence of mobile surface hydrides on ruthenium nanoparticles. *Chem. Phys. Chem.* **2005**, *6* (4), 605-607.
13. Limbach, H.-H.; Pery, T.; Rothermel, N.; Chaudret, B.; Gutmann, T.; Buntkowsky, G., Gas phase <sup>1</sup>H NMR studies and kinetic modeling of dihydrogen isotope equilibration catalyzed by Ru-nanoparticles under normal conditions: dissociative vs. associative exchange. *Phys. Chem. Chem. Phys.* **2018**.
14. Lara, P.; Ayvali, T.; Casanove, M.-J.; Lecante, P.; Mayoral, A.; Fazzini, P.-F.; Philippot, K.; Chaudret, B., On the influence of diphosphine ligands on the chemical order in small RuPt nanoparticles: combined structural and surface reactivity studies. *Dalton T.* **2013**, *42* (2), 372-82.
15. Metz, G.; Wu, X. L.; Smith, S. O., Ramped-Amplitude Cross-Polarization in Magic-Angle-Spinning Nmr. *Journal of Magnetic Resonance Series A* **1994**, *110* (2), 219-227.
16. Ross, B. D.; True, N. S., NMR spectroscopy of cyclohexane. Gas-phase conformational kinetics. *J. Am. Chem. Soc.* **1983**, *105* (15), 4871-4875.
17. Tynkkynen, T.; Hassinen, T.; Tiainen, M.; Soinen, P.; Laatikainen, R., <sup>1</sup>H NMR spectral analysis and conformational behavior of n-alkanes in different chemical environments. *Magn. Reson. Chem.* **2012**, *50* (9), 598-607.
18. Fulmer, G. R.; Miller, A. J. M.; Sherden, N. H.; Gottlieb, H. E.; Nudelman, A.; Stoltz, B. M.; Bercaw, J. E.; Goldberg, K. I., NMR Chemical Shifts of Trace Impurities: Common Laboratory Solvents, Organics, and Gases in Deuterated Solvents Relevant to the Organometallic Chemist. *Organomet.* **2010**, *29* (9), 2176-2179.

19. Anet, F. A. L.; O'Leary, D. J., H-D COUPLING-CONSTANTS AND DEUTERIUM-ISOTOPE EFFECTS ON THE PROTON CHEMICAL-SHIFTS IN PARTIALLY DEUTERIATED METHANES. *Tetrahedron Lett.* **1989**, *30* (21), 2755-2758.
20. Garrou, P. E., Transition-Metal-Mediated Phosphorus-Carbon Bond Cleavage and Its Relevance to Homogeneous Catalyst Deactivation. *Chemical Reviews* **1985**, *85* (3), 171-185.
21. Maclaughlin, S. A.; Carty, A. J.; Taylor, N. J., Hydrogenation of phosphido bridged ruthenium clusters. A view of P-C bond activation and cleavage in the coordinatively unsaturated molecule : conversion of p2-PPh<sub>2</sub> to p3-PPh. *Canadian Journal of Chemistry* **1982**, *60*, 87-90.
22. Watson, W. H.; Wu, G.; Richmond, M. G., Diphosphine Isomerization and C-H and P-C Bond Cleavage Reactivity. *Organometallics* **2006**, *25* (4), 930-945.
23. Rothermel, N.; Bouzouita, D.; Roether, T.; deRosal, I.; Tricard, S.; Poteau, R.; Gutmann, T.; Limbach, H. H.; Chaudret, B.; Buntkowsky, G., Surprising Differences of Alkane C-H Activation catalyzed by Ruthenium Nanoparticles: Complex Surface-Substrate Recognition? *Chem. Cat. Chem.* **2018**, *10*, 4243 – 4247.
24. Gutmann, T.; Bonnefille, E.; Breitzke, H.; Debouttière, P.-J.; Philippot, K.; Poteau, R.; Buntkowsky, G.; Chaudret, B., Investigation of the surface chemistry of phosphine-stabilized ruthenium nanoparticles--an advanced solid-state NMR study. *Phys. Chem. Chem. Phys.* **2013**, *15* (40), 17383-94.
25. Lara, P.; Philippot, K.; Chaudret, B., Organometallic Ruthenium Nanoparticles: A Comparative Study of the Influence of the Stabilizer on their Characteristics and Reactivity. *ChemCatChem* **2013**, *5* (1), 28-45.
26. Rafter, E.; Gutmann, T.; Loew, F.; Buntkowsky, G.; Philippot, K.; Chaudret, B.; van Leeuwen, P. W. N. M., Secondary phosphine oxides as pre-ligands for nanoparticle stabilization. *Catal. Sci. Technol.* **2013**, *3* (3), 595-599.